

# LHC bounds on MUED after Run 2 and the impact of parton shower uncertainties

Marvin M. Flores<sup>a,b</sup>, Jong Soo Kim<sup>c</sup>, Krzysztof Rolbiecki<sup>d</sup>, Roberto Ruiz de Austri Bazan<sup>e</sup>

<sup>a</sup>*Institute for Collider Particle Physics, University of the Witwatersrand, Johannesburg, South Africa*

<sup>b</sup>*National Institute of Physics, University of the Philippines, Diliman, Quezon City, Philippines*

<sup>c</sup>*National Institute for Theoretical Physics and School of Physics, University of the Witwatersrand, Johannesburg, South Africa*

<sup>d</sup>*Institute of Theoretical Physics, University of Warsaw, Warsaw, Poland*

<sup>e</sup>*Instituto de Física Corpuscular, IFIC-UV/CSIC, 46980 Paterna, Valencia, Spain*

---

## Abstract

We present the updated LHC limits on the minimal universal extra dimensions (MUED) model from the Run 2 searches. We scan the parameter space against a large number of searches implemented in the public code CHECKMATE and show that large uncertainties in the limits exist when modelling using parton showers alone due to differences in the evolution starting scale, especially in the compressed spectra. This motivates us to incorporate matching, thus deriving the most up-to-date limits on the MUED parameter space from 13 TeV searches.

---

## 1. Introduction

Over the years, the LHC collaborations have put emphasis on probing various incarnations of low energy supersymmetry (SUSY) such as minimal supergravity (mSUGRA) [1], gauge-mediated SUSY [2], anomaly-mediated SUSY [3, 4], phenomenological Minimal Supersymmetric Standard Model (pMSSM) [5], and the electroweak-MSSM [6], usually represented by simplified models. After extensively collecting data for almost a decade however, no convincing signal of supersymmetric models have been seen. This naturally led to a growing interest in various alternative beyond-the-Standard-Model (BSM) scenarios. Among these are the Universal Extra Dimensions (UED) [7] which represent a simple extension of the Standard Model (SM) that include a dark matter candidate and are also testable at the LHC. Here we focus on the minimal version, Minimal UED (MUED) [8]. The phenomenology of MUED model bears some similarities to SUSY in that each particle of the SM has a heavier Kaluza-Klein (KK) partner with the same gauge quantum. However, in contrast to SUSY, KK-particles have the same spin as their SM counterparts. The lightest particle in the KK spectrum is assumed stable and can be a dark matter candidate.

Consequently the usual collider signatures of the MUED are similar to the SUSY missing energy signatures with additional jets and leptons. The most important differences are the degenerate spectrum of a typical

MUED model and several times higher cross-section, for the same overall mass scale. The definitive differentiation between these models requires a detailed analysis of angular and invariant mass distributions of the final state products [9, 10, 11, 12, 13, 14]. Thus, SUSY searches should provide a high discovery and exclusion potential for the MUED model. Since ATLAS and CMS have performed many searches targeted at SUSY, these can be recast to provide bounds on the MUED model as was done in [15, 16, 17, 18]. In addition, non-SUSY-like searches can provide bounds as well, for example the CMS search for a di-lepton resonance at 8 TeV with  $20.6 \text{ fb}^{-1}$  which can be used to set limits on the second KK-photon [19].

A huge advantage of MUED is its predictivity and simplicity since it only depends on two parameters, the compactification radius of the extra dimension  $R$ , and a cutoff scale  $\Lambda$  at which it is replaced by a high-energy theory. The inverse compactification radius  $R^{-1}$  sets the mass scale of the first KK excitations while  $\Lambda \cdot R$  controls the allowed KK modes present in the spectrum below the cutoff. Existing bounds prior to this paper exclude models with  $R^{-1}$  values of up to 1500 GeV [16, 18].

As already mentioned, MUED spectra tend to have smaller mass splittings than supersymmetric spectra which results in softer final state products and thus decreased missing transverse energy. As a result, exclusion limits rely on initial state radiation (ISR) which provides transverse boost to the hard scattering system,

especially for low values of  $\Lambda \cdot R$ . As pointed out in Refs. [20, 21] this may result in significant QCD uncertainties when setting limits. In this Letter we explore how different settings in Monte-Carlo (MC) event generator PYTHIA 8 [22], affect constraints and their uncertainties when setting limits on the MUED parameter space. We note that this question was not considered in the earlier studies [16, 17]. Additionally, we take advantage of several ATLAS studies using full luminosity collected in Run 2. Although a thorough study of parton shower uncertainty should include a comparison of different MC event generators (e.g. HERWIG [23] or SHERPA [24]) and a variation of all parton shower parameters [25], this is beyond the scope of this work. We rather focus on the change of the parton shower scale as discussed in [26, 27].

This paper is arranged as follows: Section 2 gives a brief overview of the MUED model. Section 3 then explains the need for matching and the procedure employed to achieve this. Section 4 provides the details of the numerical simulations and analysis as well as a discussion of our bounds in the  $R^{-1}-\Lambda \cdot R$  plane.

## 2. MUED Overview

We focus on the LHC phenomenology of the first KK level excitation. In that case, each chiral SM fermion ( $Q_i, u_i, d_i, L_i, e_i$ ) (where  $i$  is the SM generation index) has one Dirac-fermion partner ( $Q_i^{(1)}, u_i^{(1)}, d_i^{(1)}, L_i^{(1)}, e_i^{(1)}$ ), each SM gauge boson  $g_\mu, W_\mu, B_\mu$  has a massive boson partner  $g_\mu^{(1)}, W_\mu^{(1)}, B_\mu^{(1)}$ , and the Higgs partner sector contains a scalar, a pseudo-scalar and a charged partner ( $h^{(1)}, A_0^{(1)}, H_\pm^{(1)}$ ). The couplings between new states are equal to the SM couplings of their partners. The masses of the KK modes are at the tree level given by

$$m_n = \sqrt{(n/R)^2 + m_{SM}^2} \quad \text{for } n \geq 1, \quad (1)$$

where  $n$  is the KK level. Since the KK modes at  $n = 1$  are the lightest, they can be abundantly produced at the LHC and will be our main focus. Equation (1) suggests a very compressed mass spectrum. However, at the loop level, the near-mass-degeneracy is partially lifted with splittings growing with  $\Lambda \cdot R$ , making the KK-gluon the heaviest state and the KK-partner of the  $U(1)_B$  gauge boson the lightest state at each KK level.

We restrict ourselves to the strong production of the colored KK-modes, i.e. KK-gluons and KK-quarks,

$$pp \rightarrow g^{(1)}g^{(1)}, pp \rightarrow Q_i^{(1)}Q_j^{(1)}, pp \rightarrow g^{(1)}Q_j^{(1)}, \quad (2)$$

where  $Q^{(1)} = Q^{(1)}, q^{(1)}$  and  $Q^{(1)}$  denotes the SU(2) doublet quark partners (or their anti-particles) and  $q^{(1)} =$

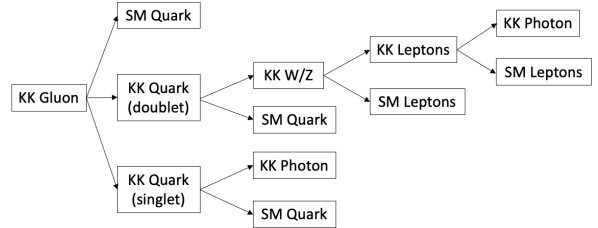


Figure 1: A typical decay chain of the KK particles following their most dominant branching ratios.

$u^{(1)}, d^{(1)}$  are the SU(2) singlet quark partners (or their anti-particles). The production of other states is suppressed by the electroweak couplings.<sup>1</sup>

The typical decay patterns of the KK-states, shown diagrammatically in Fig. 1, proceed as follows. The KK gluon is the heaviest particle and decays into KK-doublet and singlet quarks with about equal branching ratio. The KK-quark decay modes depend mainly on its SU(2) charge. The SU(2) singlet KK-quark directly decays to the KK-photon which is stable and the lightest KK particle (LKP). The SU(2) doublet KK-quarks mainly decay into the KK-gauge-bosons  $W_\pm^{(1)}$  and  $Z^{(1)}$ . The KK-W and Z bosons are lighter than the KK-quarks and so decay mostly into leptonic KK-states which in turn decay further to the LKP and a lepton. Hence, events usually have a relatively large lepton multiplicity, multiple jets, and missing transverse momentum ( $\cancel{E}_T$ ) in the final states, although all decay products can be relatively soft due to the compressed spectrum. Explicit mass spectra are shown in Table 1 for various benchmark points with  $\Lambda \cdot R = 5$  at  $\sqrt{s} = 13$  TeV.

## 3. ISR and the matching procedure

For models with compressed mass spectra, a large recoil is necessary to produce a signature with relatively low SM background. The recoil provides large missing transverse momentum (if there are heavy particles escaping detection) and gives additional transverse boost to leptons if present. The recoil is provided by the initial state radiation from incoming partons. At the MC level the ISR can be produced in the hard matrix elements or in parton shower. However, modeling ISR using a parton shower approach results in large uncertainties which are mainly due to a choice of starting scale for parton shower evolution. This is known to have a

<sup>1</sup>Although this is not the case if we consider the second KK level [19].

Table 1: The total production cross sections,  $\sqrt{s} = 13$  TeV, and mass spectra for various  $R^{-1}$  with  $\Lambda \cdot R = 5$ .

$R^{-1}$ [GeV]	Total $\sigma$ [fb]	Mass [GeV]					
		$g^{(1)}$	$Q^{(1)}$	$q^{(1)}$	$W^{(1)}/Z^{(1)}$	$L^{(1)}$	$\gamma^{(1)}$
1700	76.858	1970.48	1878.22	1854.21	1755.49	1727.33	1698.55
1800	45.614	2086.39	1988.7	1963.28	1858.54	1828.94	1798.40
1900	27.209	2202.3	2099.19	2072.35	1961.60	1930.54	1898.26
2000	16.335	2318.22	2209.67	2181.14	2064.68	2032.15	1998.11

large effect in squark and gluino production, where the uncertainty can be illustrated by varying between the “wimpy” and “power” shower settings, which respectively refers to the `SPACESHOWER:PTMAXMATCH = 1` and `SPACESHOWER:PTMAXMATCH = 2` in PYTHIA 8 [20, 28, 29].

In PYTHIA 8 for the “default” shower setting (which is `SPACESHOWER:PTMAXMATCH = 0`)  $pT_{max}$  is chosen to be the factorization scale for internal processes and the scale value for Les Houches input if the final state of the hard process (not counting subsequent resonance decays) contains at least one quark (excluding top), gluon or photon. If this is not the case, the emissions are allowed to go all the way up to the kinematical limit. This is because in the former set of processes the ISR emission of yet another quark, gluon or photon could lead to double-counting, while no such danger exists in the latter case. The “wimpy” setting, on the other hand, always uses the factorization scale for an internal process and the scale value for Les Houches input, i.e. the lower value. This avoids double-counting, but may leave out some emissions that ought to have been simulated. Finally, the “power” setting always allows emissions up to the kinematical limit which will simulate all possible event topologies, but may lead to double-counting [22].

Since MUED has a compressed spectrum especially in the low  $\Lambda \cdot R$  region of its parameter space as discussed in Section 2 and suggested by Eq. (1), we must rely on the ISR as well and therefore expect this variation when using different shower settings. This can be seen in Fig. 2 for example where production of KK gluon was done via the PYTHIA 8 setup found in the Appendix C of Ref. [18] for the benchmark point  $R^{-1} = 1700$  GeV and  $\Lambda \cdot R = 5$  with 10,000 events at 13 TeV and analysed using RIVET [30].

Therefore, if our search strategy relies on the presence of ISR, we cannot solely use parton shower simulation for determination of limits. The simulation of additional emissions at the hard matrix element level matched to the parton shower is the method that reduces the uncertainty due to ISR modelling.

Leading Jet

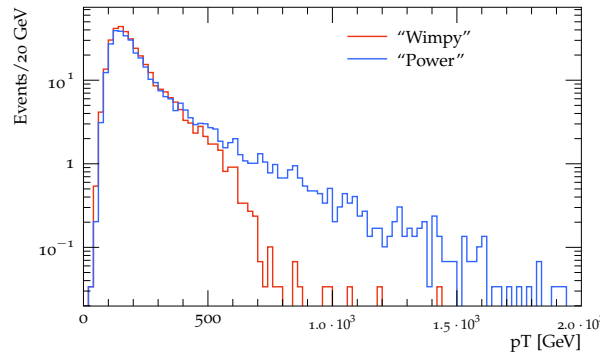


Figure 2: A comparison of the leading jet  $p_T$  distribution between the “wimpy” and “power” settings for the production of KK gluons using PYTHIA 8 for the benchmark point  $R^{-1} = 1700$  GeV and  $\Lambda \cdot R = 5$  with 10,000 events at 13 TeV normalised using an integrated luminosity of  $150 \text{ fb}^{-1}$ .

#### 4. Numerical Analysis

The samples, either with or without matching, of QCD production of KK-particles, as outlined in Section 2, are generated using MADGRAPH 5 with the UFO [31] implementation of MUED [32, 33, 34, 35] and the parton distribution function (PDF) set NN23LO1 [36, 37]. For the matched samples we use MLM matching [38] implemented in PYTHIA 8 and matrix element with up to one extra parton. The matching scale was varied in the range between  $(m_1 + m_2)/12$  and  $(m_1 + m_2)/3$ , where  $m_1$  and  $m_2$  are the masses of the final state KK-particles and the resulting cross section was stable regardless of the parton shower setting. In the following we present the results for a matching scale equal to  $(m_1 + m_2)/8$ . With these settings, we scanned the parameter space  $R^{-1}-\Lambda \cdot R$  producing 50,000 events at each grid point.

The events were then fed into CHECKMATE [39, 40, 41] for detector simulation and checked for exclusion against 30 ATLAS and 4 CMS searches, corresponding to version 2.0.30. Each analysis typically contains a large number of signal regions which target differ-

Table 2: Relevant  $\sqrt{s} = 13$  TeV analyses used in our study. The middle column denotes the target final state while the last column shows the total integrated luminosity.

Analysis	Final State	$\mathcal{L}$ [fb $^{-1}$ ]
atlas_2101_01629 [44]	$1l + \text{jets} + \cancel{E}_T$	139
atlas_conf_2019_040 [43]	$\text{jets} + \cancel{E}_T$	139
cms_sus_16_039 [45]	$\text{leptons} + \cancel{E}_T$	35.9

ent mass hierarchies and final state multiplicities. For a given search, the *best signal region* for each point in the parameter space is defined by CHECKMATE as the one with the largest *expected* exclusion potential. This criterion is then repeated to select the *best search* which is defined as the search whose *best signal region* provides the strongest exclusion. This means that the best *observed* limit is not always used but it ensures that the result is less sensitive to downward fluctuations in the data that are bound to be present when scanning over many searches and many signal regions. Once the *best search* is found for a given point in the parameter space, the signal yield in our model is then compared to the observed limit at 95% confidence level (CL),

$$r = \frac{S - 1.64 \cdot \Delta S}{S_{\text{obs}}^{95}}, \quad (3)$$

where  $S$  denotes the number of signal events,  $\Delta S$  is the  $1\text{-}\sigma$  on  $S$  combining the statistical MC uncertainty and the 10% systematic cross section uncertainty<sup>2</sup> and  $S_{\text{obs}}^{95}$  is the observed 95% CL exclusion limit. The quantity  $S - 1.64 \cdot \Delta S$  corresponds to the 95% CL lower bound on our prediction for the number of signal events, which ensures that the limits we set are conservative. The  $r$  value is only calculated for the expected best signal region. CHECKMATE does not, by default, combine signal regions nor analyses in order to optimize exclusion since the correlations between different searches and signal regions are not known in most cases. We consider a model point as excluded if  $r > 1$ .

The searches which turn out to be the most sensitive to the MUED model are atlas\_conf\_2019\_040 (2-6 jets and  $\cancel{E}_T$  at 139 fb $^{-1}$ ) [43], atlas\_2101\_01629 (1 lepton, jets and  $\cancel{E}_T$ ) [44], and cms\_sus\_16\_039 (2 same-sign leptons or at least 3 leptons plus  $\cancel{E}_T$  at 35.9 fb $^{-1}$ ) [45]. These analyses are also summarized in Table 2.

We start our numerical analysis by comparing an exclusion limit in the  $R^{-1}$ - $\Lambda \cdot R$  plane obtained for different showering settings in both matched and unmatched

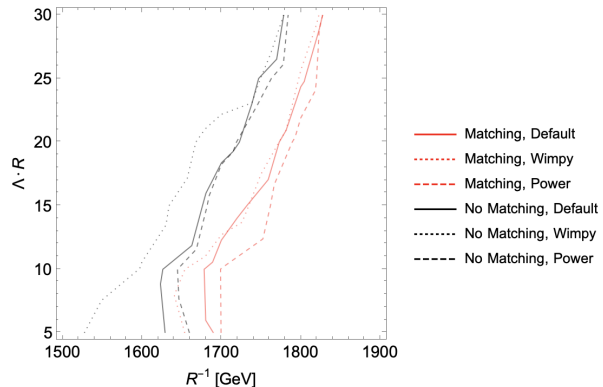


Figure 3: Limit comparison of shower-only and with matching using the “wimpy” and “power” mode. The difference is noticeable for the unmatched case at lower values of  $\Lambda \cdot R$  which corresponds to compressed mass spectrum

samples as discussed in Section 3. As can be seen in Fig. 3 for most of the parameter space the limit derived from the matched samples is stronger regardless of the shower setting. A band between power and wimpy setting can be understood as an uncertainty in the exclusion limit due to showering. As expected from the discussion in Section 3 it becomes more pronounced towards lower values of  $\Lambda \cdot R$  which correspond to more compressed mass spectra. Notably, apart from the weaker limit, the unmatched sample results in a much higher uncertainty on  $R^{-1}$  at  $\Lambda \cdot R = 5$ : 140 GeV compared with 40 GeV for a matched sample.

Figure 4 compares limits from the above mentioned searches, which have the highest sensitivity to the MUED signal. We see that the strongest limit comes from atlas\_2101\_01629 search for any value of  $\Lambda \cdot R$ . Figure 5 shows the three best signal regions that provide the strongest exclusion for this particular search. For  $\Lambda \cdot R < 10$ , the most sensitive signal region (SR) is 2J squark discovery SR (CHECKMATE label 2J\_disc\_squark) which requires at least two jets and a low- $p_T$  lepton:  $p_T > 7(6)$  GeV for electron (muon) and  $p_T < 20$  or 25 GeV, depending on a number of jets. The requirements placed on missing transverse momentum and effective mass,  $E_T^{\text{miss}} > 400$  GeV,  $m_{\text{eff}} > 1200$  GeV, enhance the sensitivity by selecting signal events with boosted final-state particles recoiling against energetic ISR jets. It is therefore well-suited for probing parameter space with low mass splitting, as it is the case for  $\Lambda \cdot R < 10$ . As we go up in  $\Lambda \cdot R$ , the sensitivity then shifts to the 4J low-x SR (CHECKMATE label 4J\_lx\_bveto\_1600) which corresponds to a higher jet multiplicity (with no  $b$ -jets) of 4 to 5, and effective mass  $m_{\text{eff}} > 1600$  GeV, which is again expected in the larger

<sup>2</sup>This approximately amounts to a size of the next-to-leading order corrections to the cross section [42].

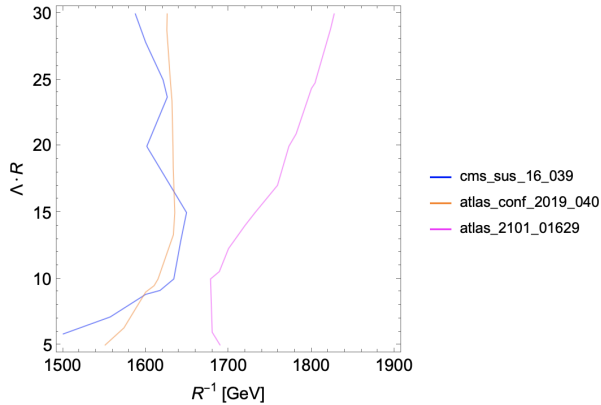


Figure 4: Exclusion plot for the searches listed in Table 2 obtained with the MLM matching and the default shower setting, as discussed in Section 4. The excluded region is to the left of the lines.

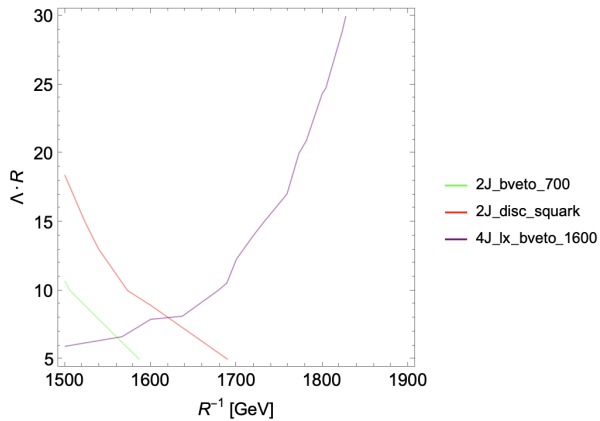


Figure 5: The most sensitive signal regions comprising the `atlas_2101_01629` search. The corresponding labels are the ones used by CHECKMATE, see text for details. The excluded region is to the left of the lines.

mass splitting region of higher  $\Lambda \cdot R$ .

It is also illuminating to look at the next two most sensitive searches just to understand the shape of exclusion lines. For the search `cms_sus_16_039`, the most sensitive signal regions are `SR_A14` (`SR_A09`) where events with three electrons or muons that form at least one opposite-sign same-flavor pair and with  $E_T^{\text{miss}} \geq 250$  GeV (200 GeV) are the strongest. Notably, the multi-lepton search using  $35.9 \text{ fb}^{-1}$  of data reaches similar sensitivity to the multi-jet search `atlas_conf_2019_040` using  $139 \text{ fb}^{-1}$ .

As already suggested, the leptonic searches can be expected to have an improved sensitivity to MUED due to the relatively large expected number of leptons in the final state compared to e.g. SUSY. Indeed, our study finds the 1-lepton search, `atlas_2101_01629`, having

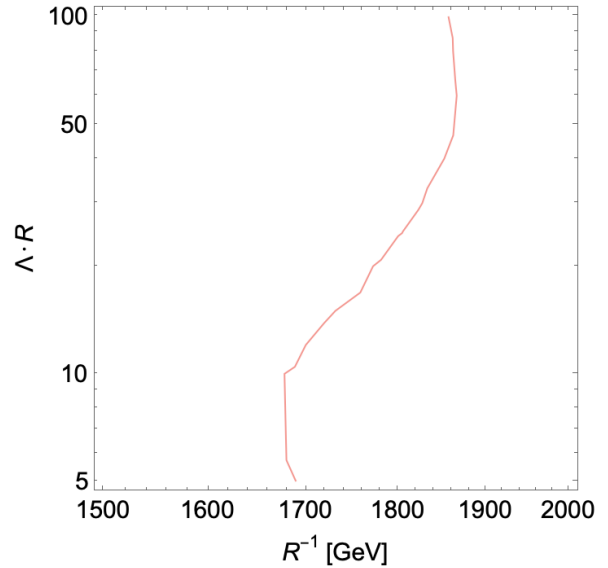


Figure 6: The combined exclusion in the minimal UED model for the matching case with the default shower setting. Note that the exclusion is entirely due to the `atlas_2101_01629` search. The excluded region is to the left of the line.

the best sensitivity in the full data set but the CMS multi-lepton search, `cms_sus_16_039` using  $\mathcal{L} = 36 \text{ fb}^{-1}$ , was also very promising and it is likely that a similar study using the full data set will be at least as sensitive as the ATLAS search. We note that in Ref. [15] it was found that same-sign/3-lepton search [46] was the most constraining for moderate to large values of  $\Lambda \cdot R$ . In our study, however, the ATLAS same-sign leptons study, `atlas_1909_08457`, was lagging behind in sensitivity. Similarly, at low  $\Lambda \cdot R$  Ref. [15] points to a search based on 2 soft leptons [47]. Again, it turns out that the full luminosity search for soft-leptons final states, `atlas_1911_12606` [48], is not as strong as the 1-lepton search `atlas_2101_01629`.

Finally, in Fig. 3 we summarize our findings. It shows the exclusion line of the MUED model for the matching case with the default shower setting. We extend the range of  $\Lambda \cdot R$  up to 100. The exclusion in  $1/R$  shows little variation at large  $\Lambda \cdot R$ , stabilizing around 1860 GeV.

In the LHC-allowed region above  $R^{-1} \sim 1700$  GeV the dark matter relic density is too high [49]. Thus, the LHC constraints together with the dark matter relic density bound essentially rule out MUED, at least for the standard cosmology.

## 5. Conclusion

We showed that in updating the limits for the MUED parameters, using parton showers alone yields large uncertainty at lower  $\Lambda \cdot R$  corresponding to a low mass spectrum. This clearly demonstrates the case for employing an appropriate matching procedure. We then updated existing limits using the current LHC searches concluding that the strongest limit comes from the `atlas_2101_01629`, which targets the final states with one lepton, jets and missing transverse energy.

## Note

We are aware of the work [50] and the discrepancies between our results and those presented therein. We are in touch with the authors in order to resolve these differences.

## Acknowledgements

MF is funded by the UP System Enhanced Creative Work and Research Grant (ECWRG-2020-2-8R). KR is supported by the National Science Centre, Poland under grants: 2016/23/G/ST2/04301, 2015/18/M/ST2/00518, 2018/31/B/ST2/02283, 2019/35/B/ST2/02008, and the Norwegian Financial Mechanism for years 2014-2021, grant DEC-2019/34/H/ST2/00707. R. RdA acknowledges partial funding/support from the Elusives ITN (Marie Skłodowska-Curie grant agreement No 674896) and the “SOM Sabor y origen de la Materia” (FPA 2017-85985-P).

## References

- [1] A. H. Chamseddine, R. L. Arnowitt and P. Nath, *Locally Supersymmetric Grand Unification*, *Phys. Rev. Lett.* **49** (1982) 970.
- [2] G. F. Giudice and R. Rattazzi, *Theories with gauge mediated supersymmetry breaking*, *Phys. Rept.* **322** (1999) 419 [[hep-ph/9801271](#)].
- [3] L. Randall and R. Sundrum, *Out of this world supersymmetry breaking*, *Nucl. Phys. B* **557** (1999) 79 [[hep-th/9810155](#)].
- [4] G. F. Giudice, M. A. Luty, H. Murayama and R. Rattazzi, *Gaugino mass without singlets*, *JHEP* **12** (1998) 027 [[hep-ph/9810442](#)].
- [5] J. A. Conley, J. S. Gainer, J. L. Hewett, M. P. Le and T. G. Rizzo, *Supersymmetry Without Prejudice at the LHC*, *Eur. Phys. J. C* **71** (2011) 1697 [[1009.2539](#)].
- [6] ATLAS collaboration, *Dark matter interpretations of ATLAS searches for the electroweak production of supersymmetric particles in  $\sqrt{s} = 8$  TeV proton-proton collisions*, *JHEP* **09** (2016) 175 [[1608.00872](#)].
- [7] T. Kakuda, K. Nishiwaki, K.-y. Oda and R. Watanabe, *Universal extra dimensions after Higgs discovery*, *Phys. Rev. D* **88** (2013) 035007 [[1305.1686](#)].
- [8] J. A. R. Cembranos, J. L. Feng and L. E. Strigari, *Minimal Universal Extra Dimensions*, in *23rd International Symposium on Lepton-Photon Interactions at High Energy (LP07)*, 8, 2007, 0708.0239.
- [9] A. J. Barr, *Determining the spin of supersymmetric particles at the LHC using lepton charge asymmetry*, *Phys. Lett. B* **596** (2004) 205 [[hep-ph/0405052](#)].
- [10] C. Athanasiou, C. G. Lester, J. M. Smillie and B. R. Webber, *Distinguishing Spins in Decay Chains at the Large Hadron Collider*, *JHEP* **08** (2006) 055 [[hep-ph/0605286](#)].
- [11] J. M. Smillie and B. R. Webber, *Distinguishing spins in supersymmetric and universal extra dimension models at the large hadron collider*, *JHEP* **10** (2005) 069 [[hep-ph/0507170](#)].
- [12] L.-T. Wang and I. Yavin, *Spin measurements in cascade decays at the LHC*, *JHEP* **04** (2007) 032 [[hep-ph/0605296](#)].
- [13] M. Burns, K. Kong, K. T. Matchev and M. Park, *A General Method for Model-Independent Measurements of Particle Spins, Couplings and Mixing Angles in Cascade Decays with Missing Energy at Hadron Colliders*, *JHEP* **10** (2008) 081 [[0808.2472](#)].
- [14] G. Moortgat-Pick, K. Rolbiecki and J. Tattersall, *Early spin determination at the LHC?*, *Phys. Lett. B* **699** (2011) 158 [[1102.0293](#)].
- [15] ATLAS collaboration, *Summary of the searches for squarks and gluinos using  $\sqrt{s} = 8$  TeV pp collisions with the ATLAS experiment at the LHC*, *JHEP* **10** (2015) 054 [[1507.05525](#)].
- [16] N. Deuschmann, T. Flacke and J. S. Kim, *Current LHC Constraints on Minimal Universal Extra Dimensions*, *Phys. Lett. B* **771** (2017) 515 [[1702.00410](#)].
- [17] D. Choudhury and K. Ghosh, *Bounds on Universal Extra Dimension from LHC Run I and II data*, *Phys. Lett. B* **763** (2016) 155 [[1606.04084](#)].
- [18] J. Beuria, A. Datta, D. Debnath and K. T. Matchev, *LHC Collider Phenomenology of Minimal Universal Extra Dimensions*, *Comput. Phys. Commun.* **226** (2018) 187 [[1702.00413](#)].
- [19] L. Edelhäuser, T. Flacke and M. Krämer, *Constraints on models with universal extra dimensions from dilepton searches at the LHC*, *JHEP* **08** (2013) 091 [[1302.6076](#)].
- [20] H. Dreiner, M. Krämer and J. Tattersall, *Exploring QCD uncertainties when setting limits on compressed supersymmetric spectra*, *Phys. Rev. D* **87** (2013) 035006 [[1211.4981](#)].
- [21] M. Drees, M. Hanussek and J. S. Kim, *Light Stop Searches at the LHC with Monojet Events*, *Phys. Rev. D* **86** (2012) 035024 [[1201.5714](#)].
- [22] T. Sjöstrand, S. Ask, J. R. Christiansen, R. Corke, N. Desai, P. Ilten et al., *An introduction to PYTHIA 8.2*, *Comput. Phys. Commun.* **191** (2015) 159 [[1410.3012](#)].
- [23] J. Bellm et al., *Herwig 7.0/Herwig++ 3.0 release note*, *Eur. Phys. J. C* **76** (2016) 196 [[1512.01178](#)].
- [24] S. Höche, S. Kuttimalai, S. Schumann and F. Siegert, *Beyond Standard Model calculations with Sherpa*, *Eur. Phys. J. C* **75** (2015) 135 [[1412.6478](#)].
- [25] S. Bornhauser, M. Drees, H. K. Dreiner and J. S. Kim, *Rapidity Gap Events in Squark Pair Production at the LHC*, *Phys. Rev. D* **80** (2009) 095007 [[0909.2595](#)].
- [26] H. K. Dreiner, M. Kramer and J. Tattersall, *How low can SUSY go? Matching, monojets and compressed spectra*, *EPL* **99** (2012) 61001 [[1207.1613](#)].
- [27] H. Dreiner, M. Krämer and J. Tattersall, *Exploring QCD uncertainties when setting limits on compressed supersymmetric spectra*, *Phys. Rev. D* **87** (2013) 035006 [[1211.4981](#)].

- [28] H. K. Dreiner, M. Kramer and J. Tattersall, *How low can SUSY go? Matching, monojets and compressed spectra*, *EPL* **99** (2012) 61001 [1207.1613].
- [29] T. Plehn, D. Rainwater and P. Z. Skands, *Squark and gluino production with jets*, *Phys. Lett. B* **645** (2007) 217 [hep-ph/0510144].
- [30] A. Buckley, J. Butterworth, D. Grellscheid, H. Hoeth, L. Lonnblad, J. Monk et al., *Rivet user manual*, *Comput. Phys. Commun.* **184** (2013) 2803 [1003.0694].
- [31] A. Alloul, N. D. Christensen, C. Degrande, C. Duhr and B. Fuks, *FeynRules 2.0 - A complete toolbox for tree-level phenomenology*, *Comput. Phys. Commun.* **185** (2014) 2250 [1310.1921].
- [32] H.-C. Cheng, K. T. Matchev and M. Schmaltz, *Bosonic supersymmetry? Getting fooled at the CERN LHC*, *Phys. Rev. D* **66** (2002) 056006 [hep-ph/0205314].
- [33] A. Datta, K. Kong and K. T. Matchev, *Minimal Universal Extra Dimensions in CalcHEP/CompHEP*, *New J. Phys.* **12** (2010) 075017 [1002.4624].
- [34] H.-C. Cheng, K. T. Matchev and M. Schmaltz, *Radiative corrections to Kaluza-Klein masses*, *Phys. Rev. D* **66** (2002) 036005 [hep-ph/0204342].
- [35] <http://feynrules.irmp.ucl.ac.be/wiki/MUED>.
- [36] NNPDF collaboration, *Parton distributions with QED corrections*, *Nucl. Phys. B* **877** (2013) 290 [1308.0598].
- [37] A. Buckley, J. Ferrando, S. Lloyd, K. Nordström, B. Page, M. Rüfenacht et al., *LHAPDF6: parton density access in the LHC precision era*, *Eur. Phys. J. C* **75** (2015) 132 [1412.7420].
- [38] M. L. Mangano, M. Moretti, F. Piccinini and M. Treccani, *Matching matrix elements and shower evolution for top-quark production in hadronic collisions*, *JHEP* **01** (2007) 013 [hep-ph/0611129].
- [39] D. Dercks, N. Desai, J. S. Kim, K. Rolbiecki, J. Tattersall and T. Weber, *CheckMATE 2: From the model to the limit*, *Comput. Phys. Commun.* **221** (2017) 383 [1611.09856].
- [40] J. S. Kim, D. Schmeier, J. Tattersall and K. Rolbiecki, *A framework to create customised LHC analyses within CheckMATE*, *Comput. Phys. Commun.* **196** (2015) 535 [1503.01123].
- [41] M. Drees, H. Dreiner, D. Schmeier, J. Tattersall and J. S. Kim, *CheckMATE: Confronting your Favourite New Physics Model with LHC Data*, *Comput. Phys. Commun.* **187** (2015) 227 [1312.2591].
- [42] A. Freitas and D. Wiegand, *QCD corrections to massive color-octet vector boson pair production*, *JHEP* **09** (2017) 058 [1706.09442].
- [43] ATLAS collaboration, *Search for squarks and gluinos in final states with jets and missing transverse momentum using 139 fb<sup>-1</sup> of  $\sqrt{s} = 13$  TeV pp collision data with the ATLAS detector*, *JHEP* **02** (2021) 143 [2010.14293].
- [44] ATLAS collaboration, *Search for squarks and gluinos in final states with one isolated lepton, jets, and missing transverse momentum at  $\sqrt{s} = 13$  TeV with the ATLAS detector*, 2101.01629.
- [45] CMS collaboration, *Search for electroweak production of charginos and neutralinos in multilepton final states in proton-proton collisions at  $\sqrt{s} = 13$  TeV*, *JHEP* **03** (2018) 166 [1709.05406].
- [46] ATLAS collaboration, *Search for supersymmetry at  $\sqrt{s} = 8$  TeV in final states with jets and two same-sign leptons or three leptons with the ATLAS detector*, *JHEP* **06** (2014) 035 [1404.2500].
- [47] ATLAS collaboration, *Search for squarks and gluinos in events with isolated leptons, jets and missing transverse momentum at  $\sqrt{s} = 8$  TeV with the ATLAS detector*, *JHEP* **04** (2015) 116 [1501.03555].
- [48] ATLAS collaboration, *Searches for electroweak production of supersymmetric particles with compressed mass spectra in  $\sqrt{s} = 13$  TeV pp collisions with the ATLAS detector*, *Phys. Rev. D* **101** (2020) 052005 [1911.12606].
- [49] J. M. Cornell, S. Profumo and W. Shepherd, *Dark matter in minimal universal extra dimensions with a stable vacuum and the “right” Higgs boson*, *Phys. Rev. D* **89** (2014) 056005 [1401.7050].
- [50] Avnish, K. Ghosh, T. Jha and S. Niyogi, *Minimal and non-minimal Universal Extra Dimension models in the light of LHC data at 13 TeV*, *Phys. Rev. D* **103** (2021) 115011 [2012.15137].